



Structure/property relationships in branched oligogermanes. Preparation of $(\text{Me}_3\text{Ge})_3\text{GePh}$, $(\text{Me}_2\text{Bu}^t\text{Ge})_3\text{GePh}$, and $(\text{Me}_2\text{PhGe})_3\text{GePh}$ and investigation of their properties by spectroscopic, spectrometric and electrochemical methods

Sangeetha P. Komanduri ^a, F. Alexander Shumaker ^a, Sydney A. Hallenbeck ^a, Cody J. Knight ^a, Claude H. Yoder ^b, Beth A. Buckwalter ^b, Craig P. Dufresne ^c, Erico J. Fernandez ^d, Christopher A. Kaffel ^d, Ryan E. Nazareno ^d, Marshall Neu ^d, Geoffrey Reeves ^d, James T. Rivard ^d, Lance J. Shackelford ^d, Charles S. Weinert ^{a,*}

^a Department of Chemistry, Oklahoma State University, Stillwater, OK 74078, USA

^b Department of Chemistry, Franklin and Marshall College, Lancaster, PA 17064-3003, USA

^c Thermo Fisher Scientific, 1400 Northpoint Parkway Suite 10, West Palm Beach, FL, 33407, USA

^d University of Detroit Jesuit High School, 8400 South Cambridge, Detroit, MI 48221, USA

ARTICLE INFO

Article history:

Received 16 June 2017

Received in revised form

17 July 2017

Accepted 18 July 2017

Available online 20 July 2017

ABSTRACT

The three branched oligogermanes $(\text{Me}_3\text{Ge})_3\text{GePh}$, $(\text{Me}_2\text{Bu}^t\text{Ge})_3\text{GePh}$, and $(\text{Me}_2\text{PhGe})_3\text{GePh}$ were synthesized via the hydrogermolysis reaction and were characterized by NMR (^1H , ^{13}C , and ^{73}Ge) spectroscopy. In addition, these three compounds and $(\text{Bu}^n\text{Ge})_3\text{GePh}$ were analyzed using high resolution accurate mass mass spectrometry (HRAM-MS), which represents the first HRAM-MS investigation of branched oligogermanes. The effects of varying the substituent pattern on the peripheral R_3Ge - groups on the electronic properties of these oligogermanes were investigated using cyclic and differential pulse voltammetry (CV and DPV), UV/visible spectroscopy, and ^{73}Ge NMR spectroscopy. The CV, DPV, and ^{73}Ge NMR data were compared to several previously reported branched oligogermanes, including $(\text{Bu}^n\text{Ge})_3\text{GePh}$, $(\text{Ph}_3\text{Ge})_3\text{GePh}$, $(\text{Ph}_3\text{Ge})_3\text{GeH}$, and $(\text{Me}_3\text{Ge})_4\text{Ge}$.

© 2017 Elsevier B.V. All rights reserved.

1. Introduction

Oligogermanes are the heavy analogues of hydrocarbons and, like their silicon- and tin-containing congeners, exhibit σ -delocalization where the electrons comprising the element – element bonds in these systems are delocalized over the chain rather than localized between only two atoms [1–11]. This occurs via overlap of the more diffuse orbitals located on the silicon, germanium, or tin atoms and in order for effective σ -delocalization to occur, the group 14 element atoms must be arranged in a *trans*-coplanar fashion. Like their lighter hydrocarbon analogs, linear, cyclic, and branched structures are known for these systems and in addition to the oligomeric molecules, polymeric systems are also known. However, in order to stabilize the substantially weaker silicon, germanium, or

tin element – element bonds, organic substituents (*n*-butyl, methyl, phenyl, etc.) are required.

The σ -delocalization present in these molecules imparts upon them interesting optical and electronic properties. In the case of germanium, these systems have been shown to function as optical and electronic materials and have even recently been suggested to function as single – molecule molecular wires [12–20]. Various methods have been used over the years to prepare discrete oligogermanes and a number of linear, cyclic, and branched species have been reported [5,8]. Our work has focused on the use of the hydrogermolysis reaction between a germanium amide R_3GeNMe_2 and a germane R_3GeH for formation of germanium – germanium single bonds. This reaction is carried out in acetonitrile at 85 °C, and involves the *in situ* formation of an α -germyl nitrile $\text{R}_3\text{GeCH}_2\text{CN}$ that is generated from the amide and the acetonitrile solvent that is the active species in the germanium – germanium bond forming process [21,22].

* Corresponding author.

E-mail address: weinert@chem.okstate.edu (C.S. Weinert).

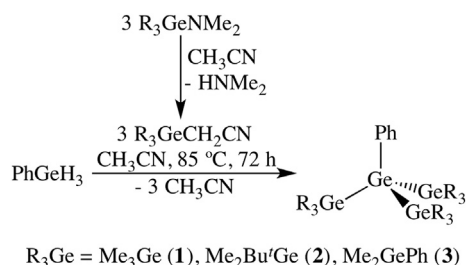
Prior to the mid-2000s branched oligogermanes were relatively rare with only a few examples having been reported in the literature. These included $(\text{Ph}_3\text{Ge})_3\text{GeR}$ ($\text{R} = \text{H}, \text{CH}_3$) [23], $(\text{Cl}_2\text{PhGe})_3\text{GePh}$ [24], $(\text{Me}_2\text{PhGe})_3\text{GePh}$ [24], $(\text{PhX}_2\text{Ge})_3\text{GePh}$ ($\text{X} = \text{OMe}, \text{SMe}, \text{Me}_2\text{N}, \text{Et}_2\text{P}$) [25], $(\text{Me}_3\text{Ge})_3\text{GeCl}$ [26], and $(\text{Me}_3\text{Ge})_4\text{Ge}$ [26–28]. The first report of a structurally characterized oligogermane $(\text{Ph}_3\text{Ge})_3\text{GePh}$ appeared in 2008 [29], and since then a number of structurally characterized branched species have been reported including $(\text{Ph}_3\text{Ge})_3\text{GeX}$ ($\text{X} = \text{H}, \text{Cl}, \text{Br}, \text{I}$) [30], the *neo*-pentyl analogs $(\text{Ph}_3\text{Ge})_4\text{Ge}$ [31], $(\text{Me}_3\text{Ge})_3\text{Ge}(\text{GePr}^i_3)$ [32], $(\text{Me}_3\text{Ge})_3\text{GeSiPr}^i_3$ [33], $(\text{Me}_3\text{Ge})_3\text{GeGe}(\text{GeMe}_3)$ [26,33], $(\text{Me}_3\text{Ge})_3\text{GeGeMe}_2\text{Ge}(\text{GeMe}_3)$ [32,33], where the latter two compounds can be regarded as mixed linear/branched species.

It has been shown through experimental and theoretical methods that both the number of catenated germanium atoms and the nature of the ancillary organic substituents affects the physical properties of these oligogermanes [15,28,30,31,34–39]. Increasing the number of catenated germanium atoms results in a red shift of the absorbance maximum in the UV/visible spectra of these systems and the presence of inductively electron donating substituents also has this effect. Additionally, these two factors affect the oxidation potential in these systems, which can be measured using both cyclic (CV) and differential pulse (DPV) voltammetry. Increasing either the number of catenated germanium atoms or the inductive electron donating ability of the side groups decreases the oxidation potential.

In both the UV/visible and electrochemical studies the variation of the degree of catenation has a more profound effect on the properties of these molecules than does variation of the organic side groups. However, variation of the substituents does still result in measurable changes in the properties of these molecules [15,34,36]. In order to investigate the substituent effects on the properties of branched oligogermanes, we have prepared and characterized the three compounds $(\text{Me}_3\text{Ge})_3\text{GePh}$ (**1**), $(\text{Me}_2\text{Bu}^t\text{Ge})_3\text{GePh}$ (**2**), and $(\text{Me}_2\text{PhGe})_3\text{GePh}$ (**3**) and have compared their voltammograms and absorbance spectra to the previously synthesized systems $(\text{Bu}^n_3\text{Ge})_3\text{GePh}$ (**4**) [40] and $(\text{Ph}_3\text{Ge})_3\text{GePh}$ (**5**) [29]. Additionally, **1–4** were also characterized by high resolution accurate mass spectrometry (HRAM-MS) and ^{73}Ge NMR spectroscopy.

2. Results and discussion

The three oligogermanes **1–3** were synthesized via the hydrogermylation reaction as shown in Scheme 1, where the amides R_3GeNMe_2 ($\text{R}_3 = \text{Me}_3, \text{Me}_2\text{Bu}^t, \text{or } \text{Me}_2\text{Ph}$) were prepared from the corresponding chlorides and LiNMe_2 . All three of the oligogermanes were pale yellow liquids at room temperature and all attempts to obtain X-ray quality crystals of these three compounds were unsuccessful. Compound **3** was previously synthesized via a different method involving the insertion of the germylene PhGeCl into the germanium–chlorine bonds of PhGeCl_3 to give



Scheme 1. Synthesis of compounds **1–3**.

$(\text{Cl}_2\text{PhGe})_3\text{GePh}$, which was subsequently treated with MeMgI to yield **3** that was isolated as a liquid [24]. The previously synthesized *n*-butyl substituted oligogermane **4** also is a liquid and did not yield crystalline material [40].

The appearance of the aryl region in the ^1H and ^{13}C NMR spectra of **1–3** is nearly identical, although the spectrum for **3** has additional peaks for the three phenyl groups on the peripheral Me_2PhGe -ligands. A peak for the protons of the *tert*-butyl groups in **2** was observed at δ 0.98 in the ^1H NMR spectrum of this compound. All three ^1H NMR spectra of **1–3** contain a singlet for the methyl groups on the peripheral ligands, and these were observed at δ 0.37 (**1**), 0.74 (**2**), and 0.27 (**3**) ppm. Similarly, the ^{13}C NMR spectra of **1–3** are very similar in the aryl region except **3** contains four additional peaks for the three peripheral phenyl groups. A resonance for the methyl carbons of the *tert*-butyl substituents in **2** appears at δ 28.3 ppm while the central carbon results in a peak at δ 26.9 ppm. Resonances for the methyl groups in these oligogermanes appear at δ 0.2 (**1**), -3.4 (**2**), and -0.2 (**3**) ppm. The resonances for **2** and **3** are shifted upfield from that of **1** due to the increase in shielding resulting from the replacement of a methyl group with a *tert*-butyl group or phenyl group, with the *tert*-butyl group providing the most shielding.

The cyclic and differential pulse voltammograms of **1–4** were obtained and are shown as overlaid plots in Fig. 1 (CV) and 2 (DPV) and values for their oxidation potentials are shown in Table 1. Experiments were carried out in CH_2Cl_2 solvent using 0.1 M $[\text{Bu}^n_4\text{N}][\text{PF}_6]$ as the supporting electrolyte and a Ag/AgCl reference electrode. These data indicate that the order of ease of oxidation is $\mathbf{4} < \mathbf{2} < \mathbf{3} < \mathbf{1}$ and the oligogermanes **1–3** each exhibit only single oxidation wave, while **4** exhibits two distinct oxidation waves.

The observed oxidation potentials in these systems can be correlated with the electron donor or acceptor properties of the substituents on the three peripheral germanium atoms. The methyl-substituted tetragermane **1** has the most positive oxidation potential at 1951 (CV) and 1650 (DPV) mV. The three methyl substituents on the peripheral Me_3Ge - groups essentially have no inductive donating properties, while the single *tert*-butyl substituent on each $\text{Me}_2\text{Bu}^t\text{Ge}$ - group in **2** is more electron donating. This can be quantified by the inductive substituent constants for these two groups, which are 0.00 for methyl and 0.300 for *tert*-butyl [41]. Therefore, the oxidation potential for **2** is less positive than that for **1** and was observed at 1782 (CV) and 1575 (DPV) mV, indicating that **2** is easier to oxidize than **1** and this is consistent with previous findings. More highly donating substituents destabilize the energy of the HOMO in these systems, and as the energy of the HOMO is destabilized the molecule is easier to oxidize [36,37,42].

The oxidation potential of the tetragermane **3** is 1877 (CV) and 1600 (DPV) mV, indicating that is intermediate between the corresponding values for **3** and **1**. The introduction of a phenyl substituent in place of a *tert*-butyl or methyl substituent introduces the possibility of π -type interactions, where the σ -bonding framework of the Ge_4 backbone can overlap with the π^* -orbitals of the phenyl ring. This has been previously reported for several linear and branched oligogermanes that show that the phenyl ring acts as both a σ -donor and π -acceptor ligand, and so its effects are twofold [30,31,34,36,37,42,43]. The inductive σ -donation of electron density from the phenyl substituent destabilizes the HOMO, while the π -acceptor interaction stabilizes the HOMO. Therefore, the σ -donor interaction renders **3** easier to oxidize than **1** but the π -acceptor interaction results in **3** being more difficult to oxidize than **2**, which contains a *tert*-butyl group that is a good σ -donor.

The oxidation potential of **4** is 1691 (CV) and 1500 (DPV) mV indicating that **4** is easier to oxidize than all three branched oligogermanes **1–3**. The electron donating ability of the three *n*-butyl substituents in **4** results in the most electron rich Ge_4 framework

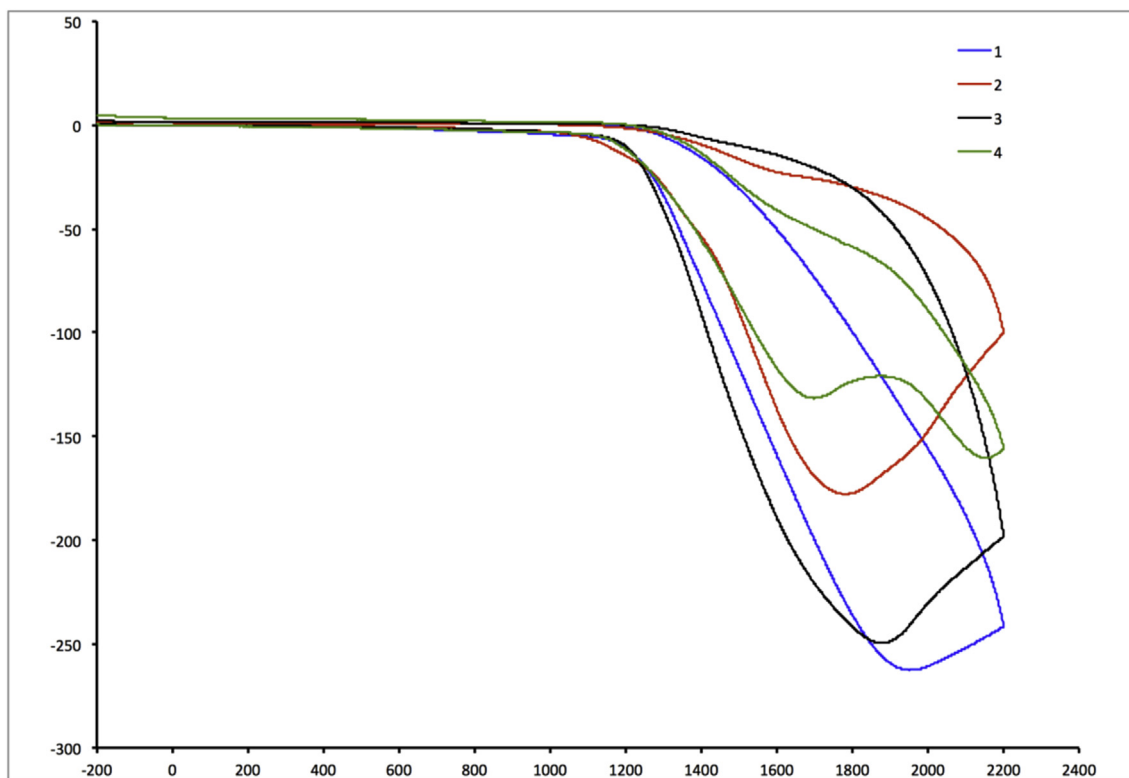


Fig. 1. Overlaid CV plot 1–4 in CH_2Cl_2 solution with 0.1 M $[\text{Bu}^n_4\text{N}][\text{PF}_6]$ as the supporting electrolyte.

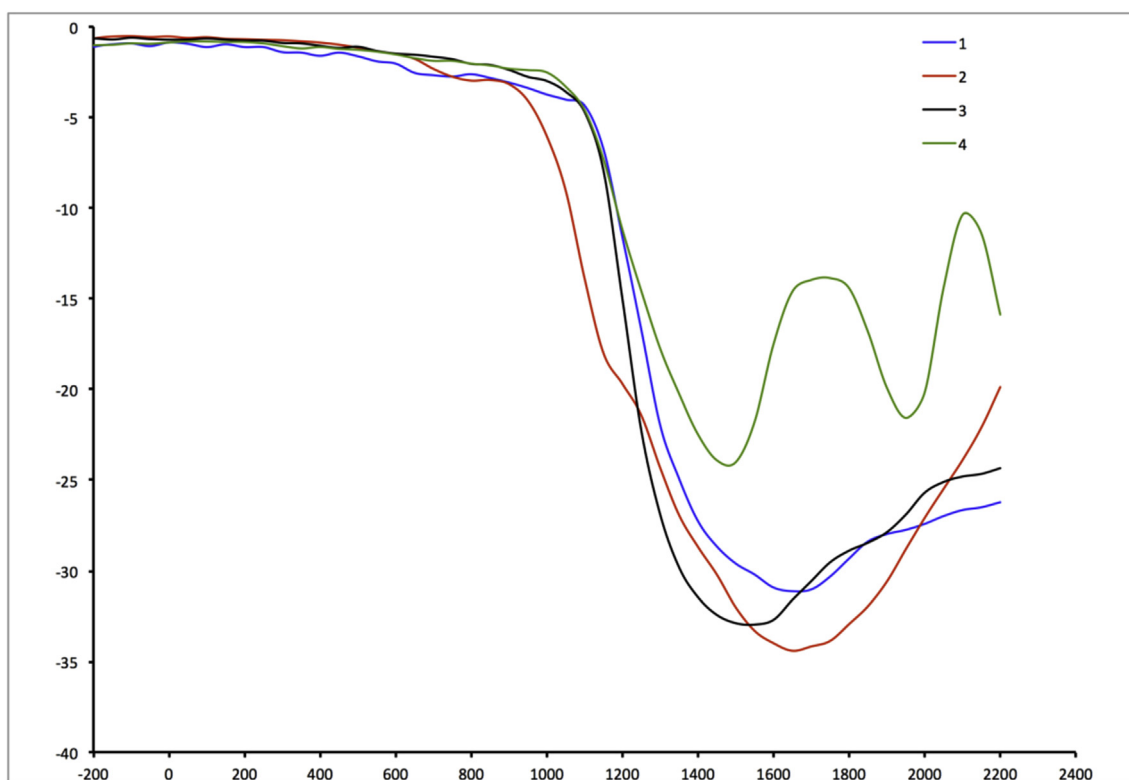


Fig. 2. Overlaid DPV plot 1–4 in CH_2Cl_2 solution with 0.1 M $[\text{Bu}^n_4\text{N}][\text{PF}_6]$ as the supporting electrolyte.

Table 1
Electrochemical data for oligogermanes 1–5.

Compound	E _{ox} (CV, mV) ^a	E _{ox} (DPV, mV) ^b
(Me ₃ Ge) ₃ GePh (1)	1951	1650
(Me ₂ Bu ^t Ge) ₃ GePh (2)	1782	1575
(Me ₂ PhGe) ₃ GePh (3)	1877	1600
(Bu ⁿ ₃ Ge) ₃ GePh (4)	1691, 2153	1500, 1950
(Ph ₃ Ge) ₃ GePh (5)	1435 ^c	1295 ^c

^a Scan rate: 50 mV/s.^b Pulse period: 0.5 s, pulse width 0.02 s, sampling time 0.01 s.^c Data from Ref. [30].

among these four compounds, and so it is expected that the oxidation potential for **4** would be the least positive. In addition, a second irreversible oxidation wave for **4** was observed at 2153 (CV) and 1950 (DPV) mV indicating the species generated after the first oxidation event takes place is stable enough to undergo further oxidation. Although multiple oxidation waves have been observed for linear oligogermanes having aryl substituents attached to the Ge – Ge backbone [31,35,44,45], this is the first example of such a pattern for a branched system.

Due to the branched configuration of **1–4**, it might be expected that the species generated after the first oxidation event occurs might be more stable than that generated after oxidation of linear oligogermanes such that a return reduction wave might be observed. Therefore, oligogermanes, **1–4** were analyzed using a microelectrode with scan rates up to 5000 mV/s, but a return reduction wave was not observed for any of these oligogermanes. Among the oligogermanes **1–5** the perphenyl-substituted derivative **5** has the least positive oxidation potential, which is 1435 (CV) and 1295 (DPV) mV [30]. The low oxidation potential for **5** is due to the σ -donor capabilities of the nine peripheral phenyl rings. Despite the presence of the phenyl substituents, analysis of **5** using a microelectrode with fast scan rates also did not result in the observation of a return reduction wave.

A second oxidation wave was not observed for **1–3** nor for **5** as was seen for **4**. Presumably, the significant inductive electron donating nature of the *n*-butyl substituents imparts stability to the product that is formed after **4** undergoes oxidation. It is likely that both linear and branched oligogermanes break apart by homolytic scission of the Ge – Ge bonds after the oxidation event takes place, and we have shown that this is what occurs in these species upon photolysis [46]. Several attempts to isolate the products being generated after oxidation failed using bulk electrolysis in the presence of acetic acid, which should trap any germanium-based radicals or germylenes that are generated after oxidation.

Bulk electrolysis experiments on **1–5** were conducted in a three-compartment cell in a 0.1 M solution of [Buⁿ₄N][PF₆] in CH₂Cl₂ in the presence of 10 M equiv. of acetic acid. The working electrode potential was held at 50 mV higher than the oxidation potential measured by CV for at least 3 h. After removal of the solvent from the reaction mixtures, the residual electrolytes were washed with hexane, the mixtures were filtered, and the hexane solvent was removed from each sample under vacuum. In each case an intractable mixture of products resulted that contained no identifiable products by ¹H NMR spectroscopy.

Alternatively, the use of CCl₄ was attempted as a trapping agent for radicals using the same experimental method. Although the final product mixture obtained from bulk electrolysis of **1–3** and **5** again contained no identifiable products, that obtained from **4** contained a significant amount of Buⁿ₃GeCl that was isolated by distillation. The ¹H and ¹³C NMR spectra of the distillate were identical to that of a commercial sample of Buⁿ₃GeCl and its identity

was further confirmed by elemental analysis. If a single Ge – Ge bond is cleaved after the first oxidation event occurs, this would result in the formation of either neutral or cationic Buⁿ₃Ge• that would then be converted to Buⁿ₃GeCl upon abstraction of a chlorine atom from CCl₄. The remaining fragment would then be either neutral or cationic (Buⁿ₃Ge)₂GePh• that might then be converted to (Buⁿ₃Ge)₂GePhCl. This trigermane fragment could then be the second species that is oxidized in the second event and then undergoes subsequent decomposition to provide two additional equivalents of Buⁿ₃GeCl (Scheme 2). It is also possible that **1–3** and **5** also decompose in a similar fashion, but the products that are generated after oxidation either polymerize or undergo rapid further decomposition.

The UV/visible spectra of **1–4** were acquired and an overlaid plot of their spectra is shown in Fig. 3 and the absorbance data is collected in Table 2. As is typical for the $\sigma \rightarrow \sigma^*$ electronic transition in oligogermanes the extinction coefficients are on the order of 10⁴ M⁻¹ cm⁻¹. It has been observed with other oligogermanes that the electronic and steric nature of the organic substituents on the germanium atoms has a measurable effect on the HOMO/LUMO gap and therefore on the position of the λ_{\max} for these compounds [30,34,36,42]. Oligogermanes **2** and **4** have the highest energy absorbance maxima at 223 and 224 nm, respectively, and therefore these two oligogermanes have the largest HOMO/LUMO gap. The trimethyl-substituted oligogermane **1** has a λ_{\max} at 237 that is red-shifted relative to those for **2** and **4** indicating that it has a larger HOMO/LUMO gap than both **2** and **4**. Oligogermane **3** has a λ_{\max} at 245 nm due to the presence of a phenyl substituent on the three peripheral germanium atoms, where the π^* -orbitals of the phenyl groups are in conjugation with the σ -bonding system of the Ge₄ backbone resulting in a decrease of the HOMO/LUMO gap.

The three branched oligogermanes **1–3** were characterized by ⁷³Ge NMR spectroscopy (Fig. 4) and their spectroscopic data, along with those for **4** [40], **5** [40], (Ph₃Ge)₃GeH (**6**) [30] and (Me₃Ge)₄Ge (**7**) [28] are collected in Table 3. This nucleus is difficult to measure since the nuclear spin is 9/2 and the resonance frequency is 17.4 MHz at a magnetic field strength of 11.743 T, resulting in significant acoustic ringing in the probe during acquisition [47–52]. However, ⁷³Ge NMR data for a number of oligogermanes have been reported and the chemical shifts for the germanium atoms have been shown to be dependent on the substituent pattern present. Resonances for trisubstituted germanium atoms R₃Ge- typically are observed between $\delta - 30$ to $- 75$ ppm, while those for disubstituted germanium atoms -R₂Ge- range from $\delta - 110$ to $- 140$ ppm and those for monosubstituted germanium atoms RGe- are further upfield between $\delta - 185$ to $- 235$ ppm.

A resonance for the central germanium atoms in **1–5** was observed in each case, and the chemical shifts range from $\delta - 188$ to $- 207$ ppm. Peaks for the central germanium atom of the trialkyl-substituted oligogermanes **1** and **4** appear the furthest downfield, at $\delta - 188$ and $- 195$ ppm, respectively. The resonances for the central germanium atom in **2** and **3** appear upfield from those in **1** and **4** at $\delta - 207$ and $- 204$ ppm, respectively, and are similar to the resonance for the central germanium atom of **5** as well [40]. The presence of aryl and branched alkyl substituents such as *tert*-butyl or *iso*-propyl has been previously shown to impart an upfield shift on the ⁷³Ge NMR resonances in linear oligogermanes as well [40,50]. The chemical shifts for the central germanium atom in **1–5** are each further downfield than those for **6** and **7**, which were observed at $\delta - 311$ and $- 339$ ppm, respectively [28,30]. The attachment of a hydrogen or a fourth trialkyl-substituted germanium atom in place of the phenyl substituents in **1–5** has a significant shielding effect [50].

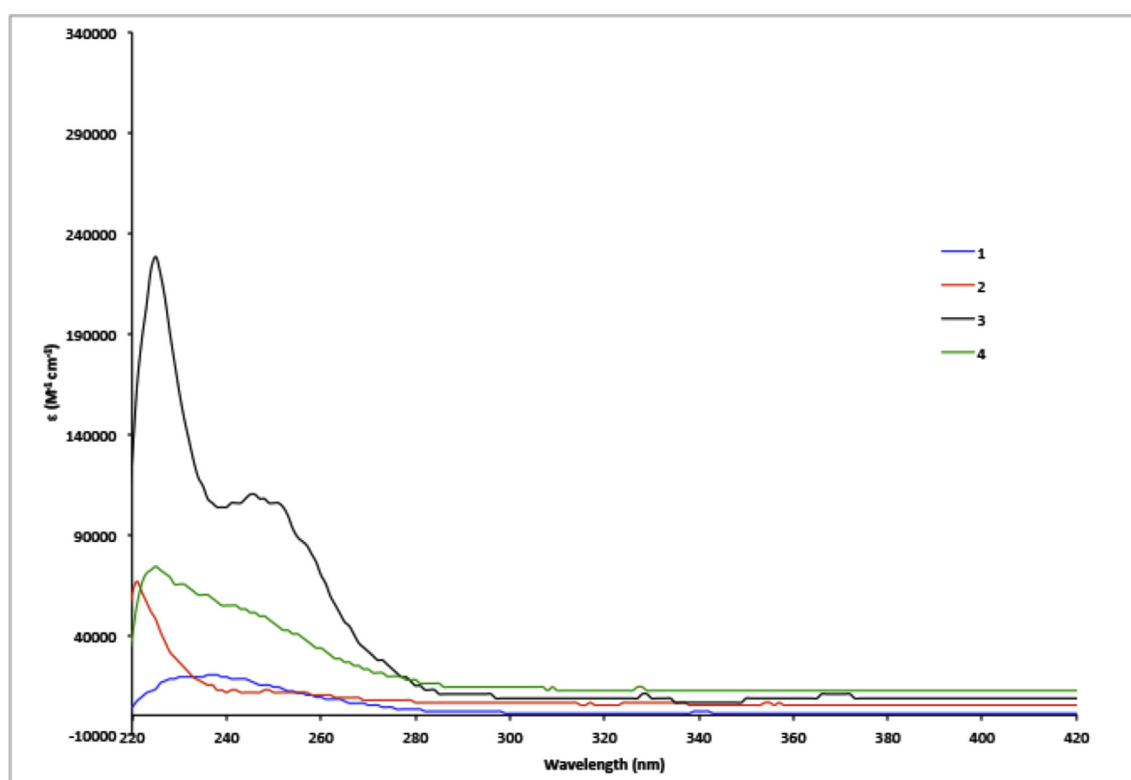
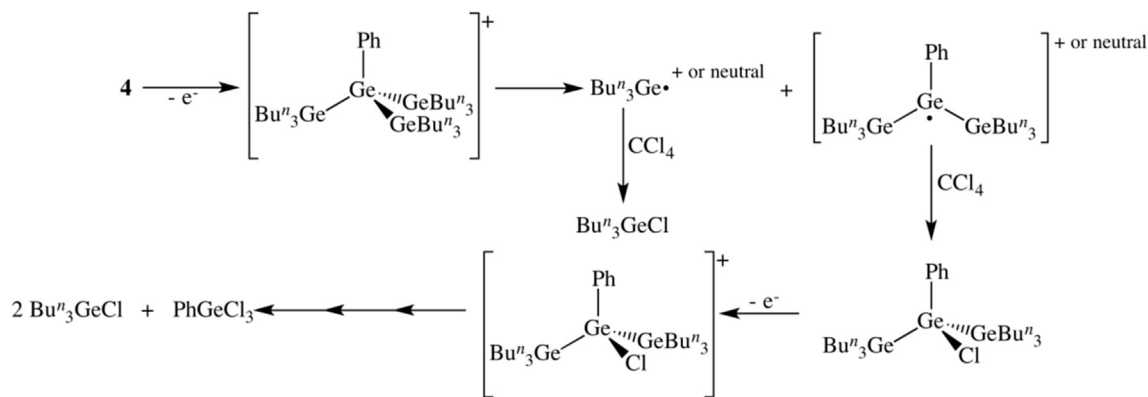


Fig. 3. Overlaid UV/visible plot for oligogermanes **1–4** in CH_2Cl_2 solution.

Table 2
UV/visible data for oligogermanes **1–4** in CH_2Cl_2 solution.

Compound	λ_{max} (nm)	ϵ ($\text{M}^{-1} \text{cm}^{-1}$)
(Me_3Ge) ₃ GePh (1)	237	2.0×10^4
($\text{Me}_2\text{Bu}^t\text{Ge}$) ₃ GePh (2)	223	5.2×10^4
(Me_2PhGe) ₃ GePh (3)	245	5.5×10^4
(Bu^n_3Ge) ₃ GePh (4)	224	7.4×10^4

Resonances were observed for the peripheral germanium atoms only in **1** and **4**. The presence of a symmetric environment about germanium is typically required in order to observe ^{73}Ge NMR resonances that are sharp enough to observe. An asymmetric environment often results in the broadening of the resonances into the baseline. Peaks for the peripheral germanium atoms in **2** and **3** were not observed due to the substituent pattern in these two

molecules. However, this also can occur in oligogermanes having germanium atoms that have three identical organic substituents, as was observed for **5**. Defined resonances for the peripheral germanium atoms in **1** and **4** were observed, where the peak at $\delta - 45$ ppm in **1** is similar to that for the Me_3Ge - groups in **7**. The resonance for the Bu^n_3Ge - groups in **4** is also in the usual region for trialkyl-substituted germanium atoms [40].

The High Resolution Accurate Mass mass spectra for compounds **1–4** were acquired, and to our knowledge these data are the first HRAM-MS studies conducted on branched oligogermanes. There are five non-radioactive isotopes of germanium and the three most abundant isotopes (^{74}Ge , ^{72}Ge , and ^{70}Ge) result in a distinct pattern in their mass spectra. The HRAM-MS data for **1–4** are collected in Table 4 and several mass spectra are shown in Fig. 5. As we have previously observed using this method [46], the parent compounds

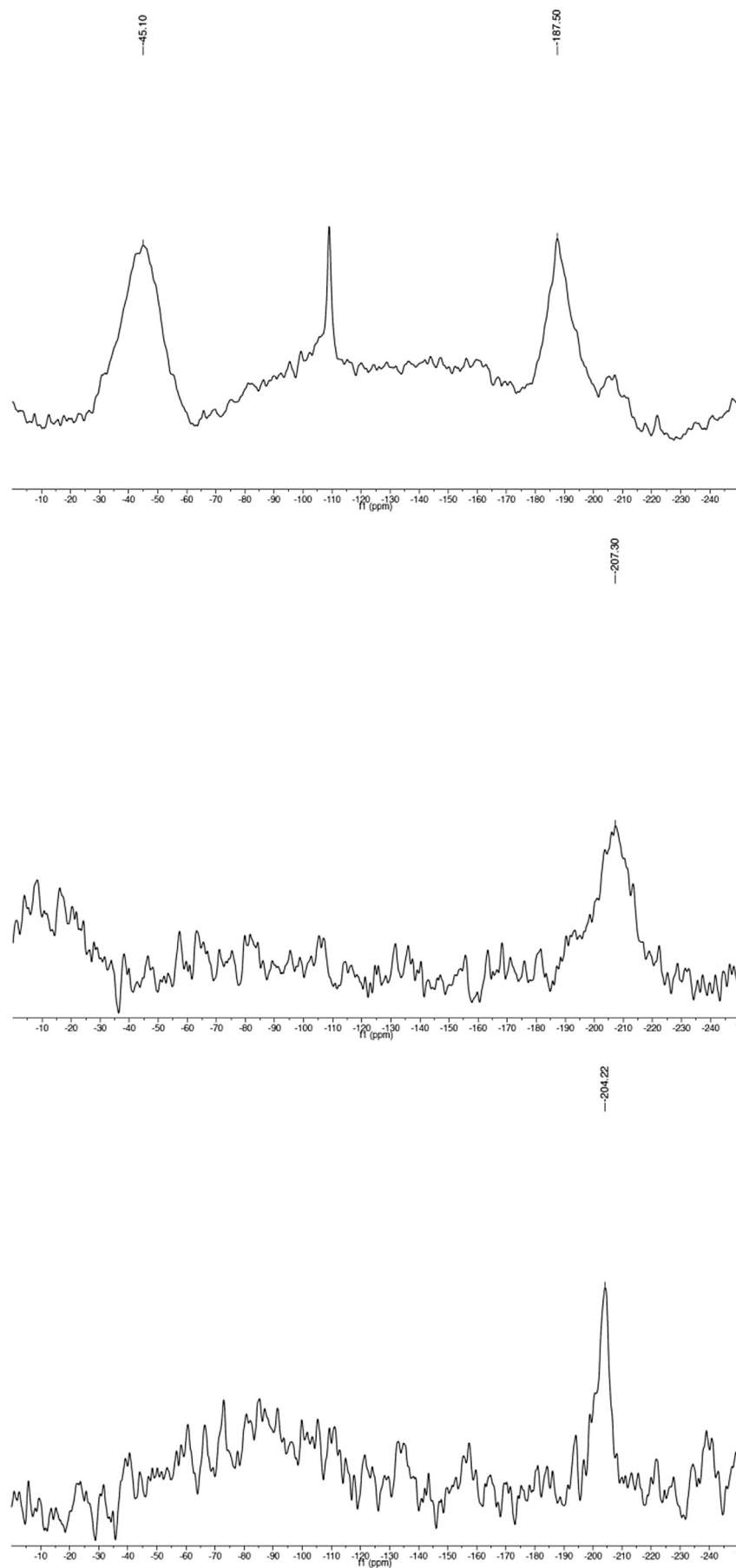


Fig. 4. ^{73}Ge NMR spectra of **1** (top), **2** (middle), and **3** (bottom) in benzene- d_6 solution. Note: The sharp line in the middle of the spectrum of **1** is an artifact.

Table 3
⁷³Ge NMR data for oligogermanes **1–5**.^a

Compound	δ –Ge _{peripheral} (ppm)	$\Delta_{1/2}$ –Ge _{peripheral} (Hz)	δ –Ge _{central} (ppm)	$\Delta_{1/2}$ –Ge _{central} (Hz)
(Me ₃ Ge) ₃ GePh (1)	– 45	296	– 188	157
(Me ₂ Bu ^t Ge) ₃ GePh (2)	n/o	n/o	– 207	296
(Me ₂ PhGe) ₃ GePh (3)	n/o	n/o	– 204	104
(Bu ⁿ ₃ Ge) ₃ GePh (4)	– 33	240	– 195	100
(Ph ₃ Ge) ₃ GePh (5)	n/o	n/o	– 202	290
(Ph ₃ Ge) ₃ GeH (6)	– 56	35	– 311	n/o ^b
(Me ₃ Ge) ₄ Ge (7)	– 38	164	– 339	9

^a n/o = not observed.^b The resonance at – 311 ppm is a doublet.**Table 4**
HRAM-MS data for oligogermanes **1–4**.

Compound	<i>m/z</i>	Assignment	Calcd. <i>m/z</i>	Error (ppm)
1	595.9871	(Me ₃ Ge) ₂ (Me ₃ GeO)GePh(CH ₃ CN)(H ₂ O) ₂ + H ⁺	595.9890	3.2
	425.9714	(Me ₃ Ge) ₂ GePh(CH ₃ CN) ⁺	425.9713	0.2
	309.9878	(Me ₃ Ge)GePh(CH ₃ CN) + H ⁺	309.9866	3.9
	160.0173	Me ₃ Ge(CH ₃ CN) ⁺	160.0176	1.9
2	670.0970	(Me ₂ Bu ^t Ge) ₃ GePh(CH ₃ CN) + H ⁺	670.1138	25.0
	551.0922	(Me ₂ Bu ^t Ge) ₂ GePh(CH ₃ CN) ₂ ⁺	551.0918	0.7
	510.0656	(Me ₂ Bu ^t Ge) ₂ GePh(CH ₃ CN) ⁺	510.0652	7.8
	352.0331	(Me ₂ Bu ^t Ge)GePh(CH ₃ CN) + H ⁺	352.0336	1.4
	243.0907	(Me ₂ Bu ^t Ge)(CH ₃ CN) ₂ ⁺	243.0911	1.6
	202.0641	(Me ₂ Bu ^t Ge)(CH ₃ CN) ⁺	202.0646	2.5
	161.0377	(Me ₂ Bu ^t Ge) ⁺	161.0380	1.9
3	782.0344	(Me ₂ PhGe) ₂ (Me ₂ PhGeO)GePh(CH ₃ CN)(H ₂ O) ₂ + H ⁺	782.0359	1.9
	377.0171	(Me ₂ PhGe) ₂ O + H ⁺	377.0176	1.3
	222.0328	Me ₂ PhGe(CH ₃ CN) ⁺	222.0333	2.3
	181.0063	Me ₂ PhGe ⁺	181.0067	2.2
4	922.3793	(Bu ⁿ ₃ Ge) ₃ GePh(CH ₃ CN) + H ⁺	922.3955	17.6
	678.2539	(Bu ⁿ ₃ Ge) ₂ GePh(CH ₃ CN) ⁺	678.2530	1.3
	528.2840	(Bu ⁿ ₃ Ge) ₂ (CH ₃ CN) ⁺	528.2840	0.1
	286.1579	Bu ⁿ ₃ Ge(CH ₃ CN) ⁺	286.1585	2.1
	245.1315	Bu ⁿ ₃ Ge ⁺	245.1319	1.6

are typically observed as adducts with acetonitrile, which is the solvent used in the measurements, and/or water that is present in trace amounts in the acetonitrile. Germoxanes are also often observed that result from the insertion of an oxygen atom into one of the Ge – Ge bonds in the oligogermane.

The HRAM-MS of **1** contains four main peaks. The parent compound is observed as a germoxane complexed with one CH₃CN molecule and two water molecules. This ion is protonated and the added proton could be attached to either a water or acetonitrile molecule, or to the oxygen atom of the germoxane. As previously observed with other oligogermanes, **1** undergoes fragmentation under the experimental conditions resulting in the observation of the (Me₃Ge)₂GePh(CH₃CN)⁺ ion due to loss of the Me₃GeO- group, the protonated (Me₃Ge)GePh(CH₃CN)H⁺ ion resulting from the loss of a Me₃Ge- group, and the Me₃Ge(CH₃CN)⁺ ion from fragmentation of all three of the peripheral Me₃Ge- groups.

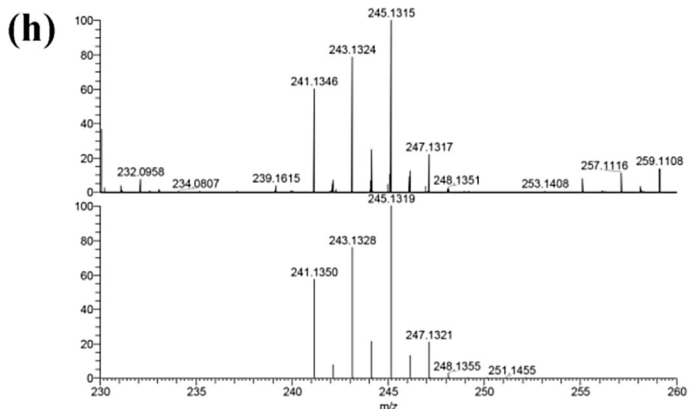
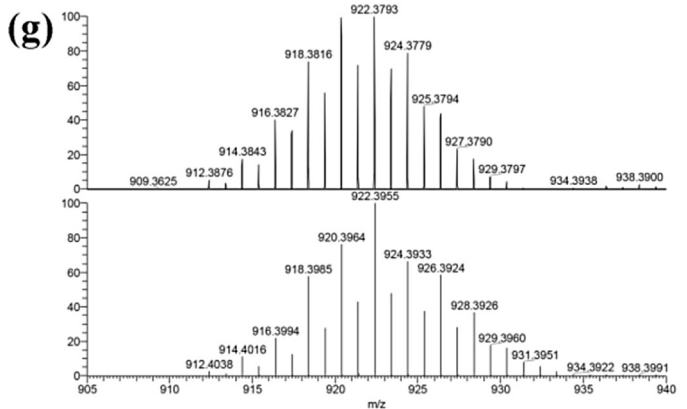
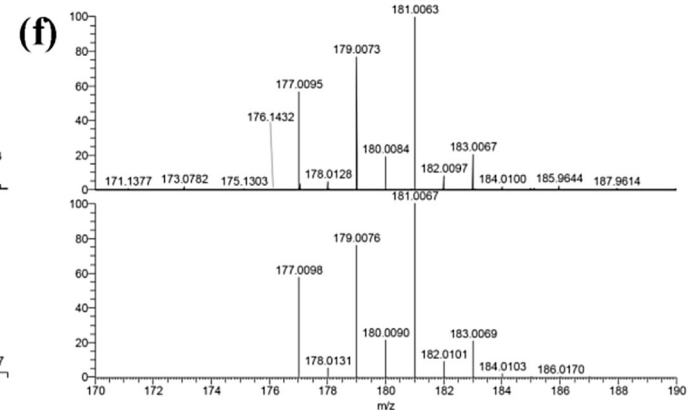
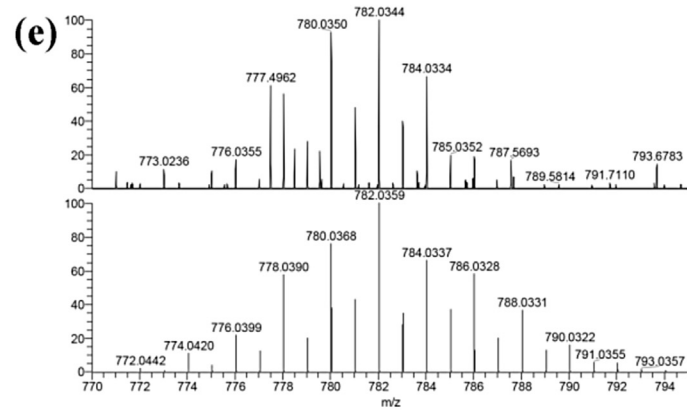
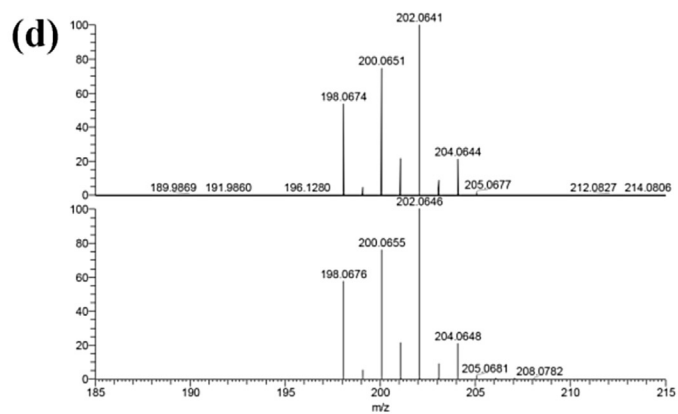
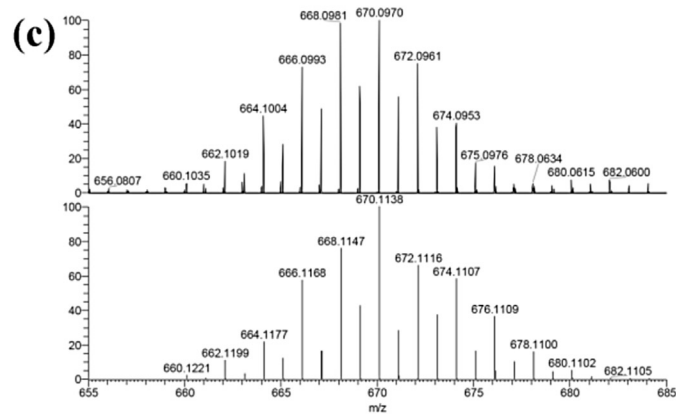
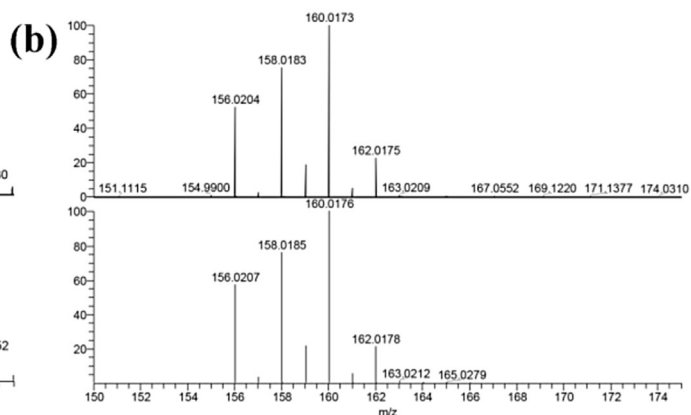
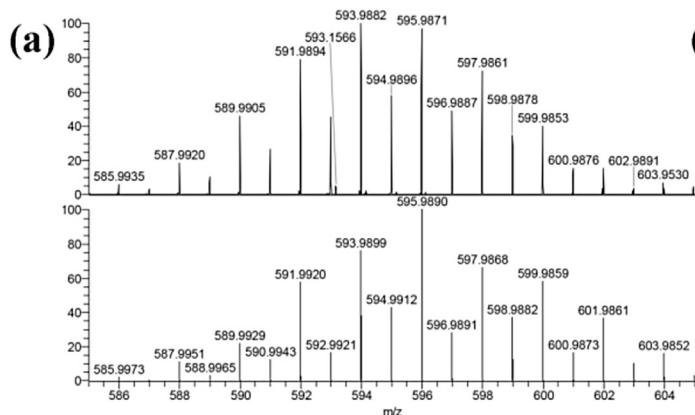
Compound **2** does not undergo oxygen insertion into a Ge – Ge bond and the parent compound was found as the protonated acetonitrile adduct (Me₂Bu^tGe)₃GePh(CH₃CN)H⁺. Fragmentation of **2** also occurred and loss of one Me₂Bu^tGe- group resulted in the formation of the (Me₂Bu^tGe)₂GePh(CH₃CN)_n⁺ ions (n = 1 or 2), while loss of a second Me₂Bu^tGe- group generated the (Me₂Bu^tGe)GePh(CH₃CN)H⁺ ion. The fragmentation of the three peripheral Me₂Bu^tGe- groups lead to the observation of the Me₂Bu^tGe(CH₃CN)_n⁺ ions (n = 1–3).

The molecular ion of **3** in its HRAM-MS was found as the protonated germoxane (Me₂PhGe)₂(Me₂PhGeO)GePh(CH₃CN)(H₂O)₂H⁺, and this fragments into the protonated digermoxane (Me₂PhGe)₂OH⁺ as well as the Me₂PhGe(CH₃CN)⁺ and Me₂PhGe⁺ ions. For **4**, the

molecular ion was observed as the protonated acetonitrile solvate (Buⁿ₃Ge)₃GePh(CH₃CN)H⁺, and this species fragments via loss of a Buⁿ₃Ge- group to yield the (Buⁿ₃Ge)₂GePh(CH₃CN)⁺ ion. Formation of the solvated digermoxane ion (Buⁿ₃Ge)₂(CH₃CN)⁺ was also observed and the peripheral tri-*n*-butyl germane groups result in the formation of the (Buⁿ₃Ge)(CH₃CN)⁺ and Buⁿ₃Ge⁺ ions.

In summary, the three branched oligogermanes (Me₃Ge)₃GePh (**1**), (Me₂Bu^tGe)₃GePh (**2**), and (Me₂PhGe)₃GePh (**3**) were synthesized using the hydrogermylation reaction and along with (Buⁿ₃Ge)₃GePh (**4**) were characterized by cyclic and differential pulse voltammetry as well as UV/visible spectroscopy. These studies indicate that variation of the substituents on the three peripheral germanium atoms imparts measurable changes in both their oxidation potentials and their absorbance spectra. Among these four oligogermanes, **4** is unique in that it exhibits two irreversible oxidation waves in both its CV and DPV while **1–3** only exhibit a single wave. Furthermore, bulk electrolysis of **4** in the presence of CCl₄ resulted in the isolation of Buⁿ₃GeCl indicating that these oligogermanes decompose by homolytic scission of the Ge – Ge bonds to generate radical species.

Oligogermanes **1–3** were characterized by ⁷³Ge NMR spectroscopy, and only in the case of **1** were resonances observed for both the peripheral and central germanium atoms, since **1** has a symmetric substitution pattern at the peripheral Ge atoms. The four oligogermanes **1–4** were also characterized by HRAM-MS and their mass spectra each show an ion corresponding to the parent compound that was observed as either an adduct with the acetonitrile solvent and/or a germoxane that results from insertion of an



oxygen atom into the Ge – Ge bonds of these species. The parent ions undergo fragmentation resulting in the observation of several daughter ions. These studies represent the first use of HRAM-MS investigations on branched oligogermanes.

3. Experimental section

3.1. General remarks

All manipulations were carried out under a nitrogen atmosphere using standard Schlenk, syringe, and glovebox techniques. Solvents were dried using a GlassCountour solvent purification system. The reagents $\text{Me}_3\text{GeNMe}_2$ [53,54], $\text{Me}_2\text{Bu}^t\text{GeNMe}_2$ [36], and $\text{Me}_2\text{PhGeNMe}_2$ [40] were prepared using literature procedures and PhGeH_3 was purchased from Gelest and used without further purification. NMR spectra were acquired using a Bruker Inova spectrometer operating at 400.00 MHz (^1H) or 100.57 MHz (^{13}C). Germanium-73 NMR spectra of the products (50 mg/mL in benzene- d_6) were recorded on a Varian INOVA 500 MHz spectrometer using a 10-mm low gamma broadband probe at 17.43 MHz with the Carr-Purcell-Maiboom-Gill (CPMG) pulse sequence [55,56] to reduce baseline roll. The following parameters were used with proton decoupling during acquisition: spectral width = 100,000 Hz, acquisition time = 0.01 s (except for compound **2**) that used 0.50 s, delay time = 0 s, line broadening factor = 20, number of transients = 1×10^6 to 1×10^7 . This pulse sequence was found to give peak widths within ca. 5% of those obtained using the standard pulse sequence up to peak widths of ca. 800 Hz. Based on multiple runs of the same sample, the error in the chemical shifts is estimated to be ± 3 ppm. The error in half-height linewidths is ca. 10%. No correction was applied to the measurement of overlapping peaks. The spectra were referenced to an external GeMe_4 sample. UV/visible spectra were obtained using an Ocean Optics Red Tide USB650UV spectrometer. Electrochemical data (CV, DPV, BE) were obtained using a Digilvy DY2312 potentiostat using a glassy carbon working electrode, a platinum wire counter electrode, and a Ag/AgCl reference electrode in CH_2Cl_2 solution using 0.1 M $[\text{Bu}_4\text{N}][\text{PF}_6]$ as the supporting electrolyte. HRAM-MS data were collected using a Thermo Fisher Q Exactive™ Hybride Quadrupole-Orbitrap™ Mass Spectrometer. Elemental analyses were conducted by Galbraith Laboratories.

3.2. Synthesis of $(\text{Me}_3\text{Ge})_3\text{GePh}$ (**1**)

In a Schlenk tube, a solution of $\text{Me}_3\text{GeNMe}_2$ (0.810 g, 5.01 mmol) in 15 mL of CH_3CN was added to PhGeH_3 (0.255 g, 1.67 mmol). The tube was sealed with a Teflon plug and the reaction mixture was heated in an oil bath at 85 °C for 72 h. The solution was transferred via cannula to a Schenk flask and the volatiles were removed *in vacuo* to yield a pale yellow/orange oil. Byproducts were removed from the crude product by distillation in a Kugelrohr oven (125 °C, 0.04 torr), which yielded **1** (0.60 g, 72%) as a pale yellow oil. ^1H NMR (C_6D_6 , 25 °C) δ 7.52 (d, $J = 7.6$ Hz, 2H, *o*- C_6H_5), 7.19–7.05 (m, 3H, *m*- C_6H_5 and *p*- C_6H_5), 0.37 (s, 27H, $-\text{CH}_3$) ppm. $^{13}\text{C}\{^1\text{H}\}$ NMR (C_6D_6 , 25 °C) δ 137.2 (*ipso*- C_6H_5), 135.8 (*o*- C_6H_5), 128.5 (*m*- C_6H_5), 127.8 (*p*-

C_6H_5), 0.2 ($-\text{CH}_3$) ppm. Anal. Calcd. for $\text{C}_{15}\text{H}_{32}\text{Ge}_4$: C, 35.80; H, 6.41. Found: C, 35.91; H, 6.38.

3.3. Synthesis of $(\text{Me}_2\text{Bu}^t\text{Ge})_3\text{GePh}$ (**2**)

In a Schlenk tube, a solution of $\text{Me}_2\text{Bu}^t\text{GeNMe}_2$ (1.60 g, 7.85 mmol) in 11 mL of CH_3CN was added to PhGeH_3 (0.390 g, 2.55 mmol). The tube was sealed with a Teflon plug and the reaction mixture was heated in an oil bath at 95 °C for 72 h. The solution was transferred via cannula to a Schenk flask and the volatiles were removed *in vacuo* to yield a pale yellow oil. Byproducts were removed from the crude product by distillation in a Kugelrohr oven (120 °C, 0.03 torr) to yield **2** (1.38 g, 86%) as a pale yellow oil. ^1H NMR (C_6D_6 , 25 °C) δ 7.51 (d, $J = 8.0$ Hz, 2H, *o*- C_6H_5), 7.17–7.03 (m, 3H, *m*- C_6H_5 and *p*- C_6H_5), 0.98 (s, 27H, $-\text{C}(\text{CH}_3)_3$), 0.74 (s, 9H, $-\text{CH}_3$) ppm. $^{13}\text{C}\{^1\text{H}\}$ NMR (C_6D_6 , 25 °C) δ 138.8 (*ipso*- C_6H_5), 136.0 (*o*- C_6H_5), 128.4 (*m*- C_6H_5), 127.8 (*p*- C_6H_5), 28.3 ($-\text{C}(\text{CH}_3)_3$), 26.9 ($-\text{C}(\text{CH}_3)_3$), -3.4 (s, $-\text{CH}_3$) ppm. Anal. Calcd. for $\text{C}_{24}\text{H}_{50}\text{Ge}_4$: C, 45.79; H, 8.01. Found: C, 45.66; H, 8.06.

3.4. Synthesis of $(\text{Me}_2\text{PhGe})_3\text{GePh}$ (**3**)

In a Schlenk tube, a solution of $\text{Me}_2\text{PhGeNMe}_2$ (1.37 g, 6.12 mmol) in 12 mL of CH_3CN was added to PhGeH_3 (0.30 g, 1.97 mmol). The tube was sealed with a teflon plug and the reaction mixture was heated in an oil bath at 95 °C for 72 h. The reaction mixture was transferred via cannula to a Schlenk flask and the volatiles were removed *in vacuo* to yield yellow oil. Byproducts were removed from the crude product by distillation in a Kugelrohr oven (130 °C, 0.02 torr) to yield **3** (1.11 g, 82%) as a pale yellow oil. ^1H NMR (C_6D_6 , 25 °C) δ 7.31–7.25 (m, 8H, *o*- $\text{C}_6\text{H}_5\text{Ge}$ and *o*- $\text{C}_6\text{H}_5\text{Me}_2\text{Ge}$), 7.12–7.05 (m, 4H, *p*- $\text{C}_6\text{H}_5\text{Ge}$ and *p*- $\text{C}_6\text{H}_5\text{Me}_2\text{Ge}$), 6.92–6.80 (m, 8H, *m*- $\text{C}_6\text{H}_5\text{Ge}$ and *m*- $\text{C}_6\text{H}_5\text{Me}_2\text{Ge}$), 0.27 (s, 18H, $-\text{CH}_3$) ppm. $^{13}\text{C}\{^1\text{H}\}$ NMR (C_6D_6 , 25 °C) δ 141.7 (*ipso*- $\text{C}_6\text{H}_5\text{Ge}$), 138.8 (*ipso*- $\text{C}_6\text{H}_5\text{Me}_2\text{Ge}$), 136.6 (*o*- $\text{C}_6\text{H}_5\text{Ge}$), 134.0 (*o*- $\text{C}_6\text{H}_5\text{Me}_2\text{Ge}$), 128.4 (*m*- $\text{C}_6\text{H}_5\text{Ge}$), 123.3 (*m*- $\text{C}_6\text{H}_5\text{Me}_2\text{Ge}$), 127.9 (*p*- $\text{C}_6\text{H}_5\text{Ge}$), 127.8 (*p*- $\text{C}_6\text{H}_5\text{Me}_2\text{Ge}$), -0.2 (s, $-\text{CH}_3$) ppm. Anal. Calcd. for $\text{C}_{30}\text{H}_{38}\text{Ge}_4$: C, 52.26; H, 5.56. Found: C, 52.15; H, 5.49.

3.5. Bulk electrolysis of $(\text{Bu}^n\text{Ge})_3\text{GePh}$ (**4**)

To a 1.0 M solution of $[\text{Bu}_4\text{N}][\text{PF}_6]$ in CH_2Cl_2 (150 mL) was added **4** (0.400 g, 0.454 mmol) and CCl_4 (2.50 g, 16.3 mmol). Under a stream of nitrogen, the mixture was transferred to a three compartment cell having a reticulated vitreous carbon electrode, a platinum wire counter electrode, and a Ag/AgCl reference electrode. The sample was electrolyzed at a potential of 2200 mV for 3 h under a stream of nitrogen. The reaction mixture was transferred to a Schlenk flask and the volatiles were removed *in vacuo*. The resulting residue was washed with hexane (2×25 mL), the mixture was filtered, and the volatiles were removed from the filtrate *in vacuo* to yield a colorless oil. The crude product mixture was distilled (275 °C, 760 torr) to yield Bu^n_3GeCl (0.20 g, 52%) as a colorless oil. The ^1H and ^{13}C NMR spectra matched that of a commercial sample (Gelest). Anal. Calcd. for $\text{C}_{12}\text{H}_{27}\text{ClGe}$: C, 51.56; H, 9.74. Found: C, 51.51; H, 9.76.

Fig. 5. HRAM-MS spectra for **1–4**.

- HRAM-MS spectrum of $(\text{Me}_3\text{Ge})_2(\text{Me}_3\text{GeO})\text{GePh}(\text{CH}_3\text{CN})(\text{H}_2\text{O})_2 + \text{H}^+$.
- HRAM-MS spectrum of $\text{Me}_3\text{Ge}(\text{CH}_3\text{CN})^+$.
- HRAM-MS spectrum of $(\text{Me}_2\text{Bu}^t\text{Ge})_3\text{GePh}(\text{CH}_3\text{CN}) + \text{H}^+$.
- HRAM-MS spectrum of $(\text{Me}_2\text{Bu}^t\text{Ge})(\text{CH}_3\text{CN})^+$.
- HRAM-MS spectrum of $(\text{Me}_2\text{PhGe})_2(\text{Me}_2\text{PhGeO})\text{GePh}(\text{CH}_3\text{CN})(\text{H}_2\text{O})_2 + \text{H}^+$.
- HRAM-MS spectrum of Me_2PhGe^+ .
- HRAM-MS spectrum of $(\text{Bu}^n_3\text{Ge})_3\text{GePh}(\text{CH}_3\text{CN}) + \text{H}^+$.
- HRAM-MS spectrum of Bu^n_3Ge^+ .

Acknowledgements

This work was supported by a research grant from the National Science Foundation (NSF), USA (Grant Number CHE-1464462) and is gratefully acknowledged.

References

- [1] V. Balaji, J. Michl, *Polyhedron* 10 (1991) 1265–1284.
- [2] R.D. Miller, J. Michl, *Chem. Rev.* 89 (1989) 1359–1410.
- [3] J.V. Ortiz, *Polyhedron* 10 (1991) 1285–1297.
- [4] R. West, *J. Organomet. Chem.* 300 (1986) 327–346.
- [5] M.L. Amadoruge, C.S. Weinert, *Chem. Rev.* 108 (2008) 4253–4294.
- [6] M. Dräger, *Rev. Silicon Germanium Tin Lead Compds.* 7 (1983) 299–445.
- [7] C.S. Weinert, *Dalton Trans.* (2009) 1691–1699.
- [8] C.S. Weinert, *Comments Inorg. Chem.* 32 (2011) 55–87.
- [9] L.R. Sita, *Organometallics* 11 (1992) 1442–1444.
- [10] L.R. Sita, *Acc. Chem. Res.* 27 (1994) 191–197.
- [11] L.R. Sita, *Adv. Organomet. Chem.* 38 (1995) 189–243.
- [12] M. Abkowitz, M. Stolka, *J. Non-Cryst. Solids* 114 (1989) 342–344.
- [13] M. Abkowitz, M. Stolka, *Solid State Commun.* 78 (1991) 269–271.
- [14] J.C. Baumert, G.C. Bjorklund, D.H. Jundt, M.C. Jurich, H. Looser, R.D. Miller, J. Rabolt, R. Sooriyakumaran, J.D. Swalen, R.J. Twieg, *Appl. Phys. Lett.* 53 (1988) 1147–1149.
- [15] W. Fa, X.C. Zeng, *Chem. Commun.* 50 (2014) 9126–9129.
- [16] T. Kodaira, A. Watanabe, O. Ito, M. Matsuda, S. Tokura, M. Kira, S. Nagano, K. Mochida, *Adv. Mater.* 7 (1995) 917–919.
- [17] Y. Matsuura, *J. Appl. Phys.* 115 (2014), 043701/043701–043701/043705.
- [18] R.D. Miller, F.M. Schellenberg, J.C. Baumert, H. Looser, P. Shukla, W. Torruellas, G.C. Bjorklund, S. Kano, Y. Takahashi, Nonlinear optical properties of substituted polysilanes and polygermanes, in: S.R. Marder, J.E. Sohn, G.D. Stucky (Eds.), *Materials for Nonlinear Optics: Chemical Perspectives* (ACS Symposium Series No. 455), American Chemical Society, Washington DC, 1991.
- [19] K. Mochida, S. Nagano, *Inorg. Chem. Commun.* 1 (1998) 289–291.
- [20] T.A. Su, H. Li, V. Zhang, M. Neupane, A. Batra, R.S. Klausen, B. Kumar, M.L. Steigerwald, L. Venkataraman, C. Nuckolls, *J. Am. Chem. Soc.* 137 (2015) 12400–12405.
- [21] M.L. Amadoruge, A.G. DiPasquale, A.L. Rheingold, C.S. Weinert, *J. Organomet. Chem.* 693 (2008) 1771–1778.
- [22] E. Subashi, A.L. Rheingold, C.S. Weinert, *Organometallics* 25 (2006) 3211–3219.
- [23] F. Glockling, K.A. Hooton, *J. Chem. Soc.* (1963) 1849–1854.
- [24] P. Rivière, J. Satgé, *Synth. Inorg. Metallorg. Chem.* 1 (1971) 13–20.
- [25] P. Rivière, J. Satgé, D. Soula, *J. Organomet. Chem.* 72 (1974) 329–338.
- [26] F. Glockling, J.R.C. Light, R.G. Strafford, *J. Chem. Soc. A* (1970) 426–432.
- [27] F. Glockling, J.R.C. Light, J. Walker, *Chem. Commun.* 1052–1053 (1968).
- [28] C.R. Samanam, N.F. Materer, C.S. Weinert, *J. Organomet. Chem.* 698 (2012) 62–65.
- [29] M.L. Amadoruge, J.A. Golen, A.L. Rheingold, C.S. Weinert, *Organometallics* 27 (2008) 1979–1984.
- [30] C.R. Samanam, M.L. Amadoruge, C.H. Yoder, J.A. Golen, C.E. Moore, A.L. Rheingold, N.F. Materer, C.S. Weinert, *Organometallics* 30 (2011) 1046–1058.
- [31] C.R. Samanam, M.L. Amadoruge, A.C. Schrick, C. Chen, J.A. Golen, A.L. Rheingold, N.F. Materer, C.S. Weinert, *Organometallics* 31 (2012) 4374–4385.
- [32] J. Hlina, R. Zitz, H. Wagner, F. Stella, J. Baumgartner, C. Marschner, *Inorg. Chim. Acta* 422 (2014) 120–133.
- [33] J. Hlina, J. Baumgartner, C. Marschner, *Organometallics* 29 (2010) 5289–5295.
- [34] M.L. Amadoruge, J.R. Gardinier, C.S. Weinert, *Organometallics* 27 (2008) 3753–3760.
- [35] M.L. Amadoruge, E.K. Short, C. Moore, A.L. Rheingold, C.S. Weinert, *J. Organomet. Chem.* 695 (2010) 1813–1823.
- [36] E.K. Schrick, T.J. Forget, K.D. Roewe, A.C. Schrick, C.E. Moore, J.A. Golen, A.L. Rheingold, N.F. Materer, C.S. Weinert, *Organometallics* 32 (2013) 2245–2256.
- [37] K.V. Zaitsev, E.K. Lermontova, A.V. Churakov, V.A. Tafeenko, B.N. Tarasevich, O.K. Poleshchuk, A.V. Kharcheva, T.V. Magdesieva, O.M. Nikitin, G.S. Zaitseva, S.S. Karlov, *Organometallics* 34 (2015) 2765–2774.
- [38] H. Kawabata, K. Matsushige, S. Ohmori, H. Tachikawa, *Mol. Cryst. Liq. Cryst.* 472 (2007) 297–305.
- [39] S.P. Komanduri, F.A. Shumaker, K.D. Roewe, M. Wolf, F. Uhlig, C.E. Moore, A.L. Rheingold, C.S. Weinert, *Organometallics* 35 (2016) 3240–3247.
- [40] M.L. Amadoruge, C.H. Yoder, J.H. Conneywerdy, K. Heroux, A.L. Rheingold, C.S. Weinert, *Organometallics* 28 (2009) 3067–3073.
- [41] P. Hanson, *J. Chem. Soc. Perkin Trans. II* (1984) 101–108.
- [42] K.V. Zaitsev, K. Lam, Z. Zhanabil, Y. Suleimen, A.V. Kharcheva, V.A. Tafeenko, Y.F. Oprunenko, O.K. Poleshchuk, E.K. Lermontova, A.V. Churakov, *Organometallics* 36 (2017) 298–309.
- [43] K. Zaitsev, A.A. Kapranov, Y.F. Oprunenko, A.V. Churakov, J.A.K. Howard, B.N. Tarasevich, S.S. Karlov, G.S. Zaitseva, *J. Organomet. Chem.* 700 (2012) 207–213.
- [44] K.D. Roewe, J.A. Golen, A.L. Rheingold, C.S. Weinert, *Can. J. Chem.* 92 (2014) 533–541.
- [45] K.D. Roewe, A.L. Rheingold, C.S. Weinert, *Chem. Commun.* 49 (2013) 8380–8382.
- [46] S.P. Komanduri, A.C. Schrick, C.L. Feasley, C.P. Dufresne, C.S. Weinert, *Eur. J. Inorg. Chem.* (2016) 3196–3203.
- [47] C.S. Weinert, *ISRN Spectroscopy* (2012). Article ID 718050, 718018 pp.
- [48] A.L. Wilkins, P.J. Watkinson, K.M. Mackay, *J. Chem. Soc., Dalton Trans.* (1987) 2365–2372.
- [49] K.M. MacKay, R.A. Thomson, *Main Group Met. Chem.* 10 (1987) 83–108.
- [50] Y. Takeuchi, T. Takayama, *Annu. Rep. NMR Spectro.* 54 (2005) 155–200.
- [51] P.J. Watkinson, K.M. MacKay, *J. Organomet. Chem.* 275 (1984) 39–42.
- [52] E. Liepins, I. Zicmane, E. Lukevics, *J. Organomet. Chem.* 341 (1988) 315–333.
- [53] P.J. Cordiero, T.D. Tilley, *Langmuir* 27 (2011) 6295–6304.
- [54] J. Mack, C.H. Yoder, *Inorg. Chem.* 8 (1969) 278–281.
- [55] H.Y. Carr, E.M. Purcell, *Phys. Rev.* 94 (1954) 630–638.
- [56] S. Meiboom, D. Gill, *Rev. Sci. Instrum.* 29 (1958) 688–691.